

Preclinical studies of novel therapies for Epstein-Barr virus-associated diseases in humanized mouse models (ポスター)	Imadome K, Matsuda G, Kawano F, Kodama E, Arai A, Shimizu N, Fujiwara S.	39th Annual International Herpesvirus Workshop	20-23 July, 2014	国内
The highly conserved human cytomegalovirus UL136 ORF generates multiple Golgi-likalizing protein isoforms through differential translation initiation (ポスター)	Liao H, Lee J-H, Kondo R, Katata M, Imadome K, Miyado K, Inoue N, Fujiwara S, Nakamura H.	39th Annual International Herpesvirus Workshop	20-23 July, 2014	国内
Anti-tumor effects of suberoylanilide hydroxamic acid on Epstein-Barr virus-associated T- and natural killer-cell lymphoma. (口頭)	Siddiquey M, Nakagawa H, Iwata S, Kanazawa T, Suzuki M, Imadome K, Fujiwara S, Goshima F, Murata T, Kimura H.	39th Annual International Herpesvirus Workshop	20-23 July, 2014	国内
STAT3 is activated by EBV in EBV-T/NK-LPDs leading to development of the disorders (口頭)	Komatsu H, Imadome K-I, Shibayama H, Yada T, Yamada M, Yamamoto K, Koyama T, Fujiwara S, Miura O, Arai A.	American Society of Hematology Annual Meeting,	6-Dec-14	国外
Human Osteoclasts are Mobilized in Erosive Arthritis of Epstein-Barr Virus-infected Humanized NOD/Shi-scid/IL-2R γ null Mice (ポスター)	Nagasawa Y, Natsumi I, Nozaki T, Inomata H, Imadome K-I, Iwata M, Kitamura N, Fujiwara S, Takei M.	American College of Rheumatology Annual meeting	November 14-19, 2014	国内
DNAメチル化阻害剤ゼブラリンのヒト胆管癌細胞に対する抗腫瘍活性(ポスター)	中村和昭、中林一彦、Kyaw Htet Aung、秦健一郎、田上昭人	分子生物学会	2014/12/1	国内
PVRL1遺伝子変異を認めたcleft lip/palate-ectodermal dysplasiaの一例(口頭)	吉田和恵、藤田秀樹、久保田雅也、下村裕、新関寛徳	第38回小児皮膚科学会、東京	2014/7/5	国内
無汗性外胚葉形成不全症の一例(口頭)	栗原佑一、渡邊絵美子、宮川俊一、梶原久美子、新関寛徳	第38回小児皮膚科学会、東京	2014/7/5	国内
難治性下腿潰瘍を合併した肥厚性皮膚骨膜炎の1例(口頭)	中澤慎介、森 達吉、新関寛徳、戸倉新樹	第110回日本皮膚科学会静岡地方会、三島市	2014/10/18	国内
肥厚性皮膚骨膜炎の1例	皆川智子、金子高英、中野 創、澤村大輔、水上浩哉、斎藤陽子、二川原健、新関寛徳	第368回日本皮膚科学会青森地方会、弘前市	2014/11/16	国内
難治性下腿潰瘍を合併した肥厚性皮膚骨膜炎の1例(口頭)	中澤慎介、森 達吉、新関寛徳、戸倉新樹	第38回皮膚脈管膠原病研究会、東京	2015/1/30	国内

Mutations in SERPINB7, encoding a serine protease inhibitor, cause Nagashima-type palmoplantar keratosis (ポスター発表)	Kubo A, Shiohama A, Sasaki T, Nakabayashi K, Kosaki K, Kudoh J, Hata K, Umezawa A, Tokura Y, Ishiko A, Niizeki H, Kabashima K, Mitsuhashi Y, Amagai M.	74th Annual Meeting Society for Investigative Dermatology, New Mexico	2014/5/10	国外
長島型掌蹠角化症の原因遺伝子SERPINB7の同定と患者30例の変異解析(口頭発表)	久保亮治, 塩濱愛子, 佐々木貴史, 中林一彦, 奥山虎之, 小崎健次郎, 工藤純, 秦健一郎, 梅澤明弘, 戸倉新樹, 石河晃, 新関寛徳, 梶島健治, 三橋善比古, 天谷雅行	第113回日本皮膚科学会総会, 京都	2014/5/31	国内
KRT5に新規遺伝子変異を認めた色素異常型単純型表皮水疱症の親子例(口頭発表)	熊谷宜子, 中村善雄, 佐々木貴史, 高橋勇人, 天谷雅行, 久保亮治	第854回日本皮膚科学会東京支部地方会, 東京	2014/6/21	国内
片側性に列序性表皮母斑と掌蹠角化を認めたCostello症候群の体細胞モザイクの一例(口頭発表)	本多皓, 佐々木貴史, 中林一彦, 秦健一郎, 谷川瑛子, 久保亮治	第38回日本小児皮膚科学会学術大会, 東京	2014/7/5	国内
消化管穿孔を繰り返したテネインX欠損によるエーラス・ダンロス症候群の1例(口頭発表)	崎山とも, 種本紗枝, 布袋祐子, 松本健一, 久保亮治	2014年度日本皮膚科学会合同臨床東京地方会, 東京	2014/7/12	国内
長島型掌蹠角化症の1例～遺伝子解析を含めて～(口頭発表)	仁木真理子, 広瀬憲志, 森谷眞紀, 塩濱愛子, 久保亮治	第29回角化症研究会, 東京	2014/8/2	国内
Dowling-Meara型単純型表皮水疱症の1例(口頭発表)	田中博子, 吉田憲司, 根岸亜津佐, 石井健, 江藤宏夫, 佐々木貴史, 久保亮治, 石河晃	第856回日本皮膚科学会東京地方会, 東京	2014/9/20	国内
A novel frameshift mutation of c.1638_1641delCAGT in KRT5 in a Japanese family with epidermolysis bullosa simplex with mottled pigmentation (ポスター発表)	Kumagai Y, Nakamura Y, Sasaki T, Takahashi H, Amagai M, Kubo A	Eastern Asia Dermatology Congress (EADC2014), Korea	2014/10/25	国外
長島型掌蹠角化症の1例	中野敏明, 善家由香理, 西川沙織, 中村仁美, 新井達, 衛藤光, 三橋善比古, 久保亮治	第857回日本皮膚科学会東京地方会, 東京	2014/11/15	国内
9番染色体上のLMX1B遺伝子領域に染色体微小欠失を認めたNail-Patella症候群の母娘例	向井美穂, 安田文世, 伏間江貴之, 谷川瑛子, 天谷雅行, 久保亮治	第857回日本皮膚科学会東京地方会, 東京	2014/11/15	国内
Pallister-Killian症候群の1例～伊藤白斑との関連について～	小野紀子, 久保亮治, 天谷雅行, 松井順子, 小崎健次郎, 田中勝	第857回日本皮膚科学会東京地方会, 東京	2014/11/15	国内

2. 学会誌・雑誌等における論文掲載

掲載した論文(発表題目)	発表者氏名	発表した場所 (学会誌・雑誌 等名)	発表した時 期	国内・ 外の別
TBX1 mutation identified by exome sequencing in a Japanese family with 22q11.2 deletion syndrome-like craniofacial features and hypocalcemia.	Ogata T, Niihori T, Tanaka N, Kawai M, Nagashima T, Funayama R, Nakayama K, Nakashima S, Kato F, Fukami M, Aoki Y, Matsubara Y	PLoS One.	2014	国外
Seven Novel Mutations in Bulgarian Patients with Acute Hepatic Porphyrias (AHP).	Dragneva S, Szyszka-Niagolov M, Ivanova A, Mateva L, Izumi R, Aoki Y, Matsubara Y.	JIMD Rep.	2014	国外
New BRAF knockin mice provide a pathogenetic mechanism of developmental defects and a therapeutic approach in cardio-facio-cutaneous syndrome.	Inoue SI, Moriya M, Watanabe Y, Miyagawa-Tomita S, Niihori T, Oba D, Ono M, Kure S, Ogura T, Matsubara Y, Aoki Y.	Hum Mol Genet.	2014	国外
GNE myopathy associated with congenital thrombocytopenia: A report of two siblings.	Izumi R, Niihori T, Suzuki N, Sasahara Y, Rikiishi T, Nishiyama A, Nishiyama S, Endo K, Kato M, Warita H, Konno H, Takahashi T, Tateyama M, Nagashima T, Funayama R, Nakayama K, Kure S, Matsubara Y, Aoki Y, Aoki M.	Neuromuscul Disord.	2014	国外
Targeted Next-Generation Sequencing Effectively Analyzed the Cystic Fibrosis Transmembrane Conductance Regulator Gene in Pancreatitis.	Nakano E, Masamune A, Niihori T, Kume K, Hamada S, Aoki Y, Matsubara Y, Shimosegawa T.	Dig Dis Sci.	2014	国外
A novel heterozygous MAP2K1 mutation in a patient with Noonan syndrome with multiple lentigines.	Nishi E, Mizuno S, Nanjo Y, Niihori T, Fukushima Y, Matsubara Y, Aoki Y, Kosho T.	Am J Med Genet A.	2014	国外
Molecular basis of non-syndromic hypospadias: systematic mutation screening and genome-wide copy-number analysis of 62 patients.	Kon M, Suzuki E, Dung VC, Hasegawa Y, Mitsui T, Muroya K, Ueoka K, Igarashi N, Nagasaki K, Oto Y, Hamajima T, Yoshino K, Igarashi M, Kato-Fukui Y, Nakabayashi K, Hayashi K, Hata K, Matsubara Y, Moriya K, Ogata T, Nonomura K, Fukami M.	Hum Reprod.	2015	国外
Compilation of copy number variants identified in phenotypically normal and parous Japanese women.	Migita O, Maehara K, Kamura H, Miyakoshi K, Tanaka M, Morokuma S, Fukushima K, Shimamoto T, Saito S, Sago H, Nishihama K, Abe K, Nakabayashi K, Umezawa A, Okamura K, Hata K.	J Hum Genet	2014;59:326-331	国内
Mutation spectrum and phenotypic variation in nine patients with SOX2 abnormalities.	Suzuki J, Azuma N, Dateki S, Soneda S, Muroya K, Yamamoto Y, Saito R, Sano S, Nagai T, Wada H, Endo A, Urakami T, Ogata T, Fukami M	J Hum Genet	2014/6	国外

Rapid generation of mouse models with defined point mutations by the CRISPR/Cas9 system.	Inui M, Miyado M, Igarashi M, Tamano M, Kubo A, Yamashita S, Asahara H, Fukami M, Takada S	Sci Rep	2014/6	国外
Skeletal deformity associated with SHOX deficiency.	Seki A, Jinno T, Suzuki E, Takayama S, Ogata T, Fukami M	Clin Pediatr Endocrinol	2014/7	国外
Anti-tumor effects of suberoylanilide hydroxamic acid on Epstein-Barr virus-associated T- and natural killer- cell lymphoma	Siddiquey MN, Nakagawa H, Iwata S, Kanazawa T, Suzuki M, Imadome KI, Fujiwara S, Goshima F, Murata T, Kimura H.	Cancer Sci	2014; 105(6):713-22.	国外
CD137 expression is induced by Epstein-Barr virus infection through LMP1 in T or NK cells and mediates survival promoting signals.	Yoshimori M, Imadome KI, Komatsu H, Wang L, Saitoh Y, Yamaoka S, Fukuda T, Kurata M, Koyama T, Shimizu N, Fujiwara S, Miura O, Arai A.	PLoS ONE	2014 Nov 19;9(11):e12564.	国外
Modeling EBV infection and pathogenesis in new-generation humanized mice	Fujiwara S, Imadome K, and Takei M.	Exp Mol Med	47, e136; doi:10.1038/emm.2014.102 Published online 23 January 2015	国外
Interstitial Lung Disease with Multiple Microgranulomas in Chronic Granulomatous Disease.	Kawai T, Watanabe N, Yokoyama M, Nakazawa Y, Goto F, Uchiyama T, Higuchi M, Maekawa T, Tamura E, Nagasaka S, Hojo M, Onodera M	J Clin Immunol	2014;34: 933-940	国外
Augmentation of anti-tubercular therapy with interferon g in a patient with dominant partial interferon g.	Takeda K, Nakazawa Y, Komuro H, Yamamoto M, Shoji K, Morita K, Miyairi I, Katsuta T, Ohya Y, Ishiguro A, Onodera M	Clinical Immunology	2014;151: 25-28	国外

機関名 東北大学

1. 学会等における口頭・ポスター発表

発表した成果(発表題目、口頭・ポスター発表の別)	発表者氏名	発表した場所(学会等名)	発表した時期	国内・外の別
ヌーナン症候群の新規原因遺伝子RIT1の同定(口頭発表)	青木洋子、新堀哲也、岡本伸彦、水野誠司、黒澤健司、緒方勤、井上晋一、松原洋一	第117回日本小児科学会学術集会(名古屋)	2014/4/11-13	国内
Molecular analysis of RASopathies using next generation sequencer (口頭発表)	Aoki Y, Niihori T, Inoue SI and Matsubara Y	The 14 th East Asian Union of Human Genetics (EAUHGS) Annual Meeting (Tokyo)	2014/11/20	国内

次世代シーケンサーを用いた希少遺伝性疾患の遺伝子解析研究の現状（口頭発表）	青木洋子	日本人類遺伝学会第59回大会（東京）	2014/11/19-22	国内
新規BRAFノックインマウスの作製によるcardio-facio-cutaneous症候群の病態解明と治療法研究（口頭発表）	井上晋一、守谷充司、渡邊裕介、宮川一富田幸子、新堀哲也、大場大樹、小野栄夫、呉繁夫、小椋利彦、松原洋一、青木洋子	日本人類遺伝学会第59回大会（東京）	2014/11/19-22	国内
BRAF knock-in mice provide a pathogenetic mechanism of developmental defects and a therapeutic approach in RASopathies（口頭発表）	井上晋一、守谷充司、渡邊裕介、宮川一富田幸子、新堀哲也、大場大樹、小野栄夫、呉繁夫、小椋利彦、松原洋一、青木洋子	第37回日本分子生物学会年会（横浜）	2014/11/25-27	国内
H3K27メチル化に先立って転写は抑制される（口頭）	中山 啓子	東京（新学術領域研究 細胞運命制御 第5回領域会議）	2012/9/2	国内
がん遺伝子による転写変化とエピゲノム変化（口頭）	中山 啓子	長崎（第23回長崎障害者支援再生医療研究会）	2012/11/4	国内
マウスES細胞におけるgemininの細胞周期と分化に対する制御（ポスター）	福本恵美子, Kundu, Lena Rani, 佐藤聡一郎, 細金正樹, 中山啓子	横浜（第37回日本分子生物学会年会）	2012/11/27	国内
H3K27me3修飾パターン形成過程の時系列解析（ポスター）	細金正樹, 舟山亮, 城田松之, 中山啓子	横浜（第37回日本分子生物学会年会）	2012/11/25	国内
精子形成におけるE3ユビキチンリガーゼβ-TrCPの新規基質の同定と解析（ポスター）	久志瞭, 中川直, 中野星児, 遠藤尚博, 中山啓子	横浜（第37回日本分子生物学会年会）	2012/11/27	国内
TFIID complex changes accompany epithelial-mesenchymal transition (EMT)（ポスター）	Nakagawa, Tadashi Nakayama, Keiko	横浜（第37回日本分子生物学会年会）	2012/11/25	国内
次世代シーケンサーを用いた膵炎関連遺伝子の解析（口演）	中野絵里子、正宗 淳、桑 潔、下瀬川徹.	第100回日本消化器病学会総会.	2014/4/26	国内
次世代シーケンサーを用いた膵炎患者におけるカルシウム感知受容体遺伝子変異の解析.	中野絵里子、正宗 淳、桑 潔、下瀬川徹.	第45回日本膵臓学会大会	2014/7/12	国内
次世代シーケンサーを用いた希少遺伝性難病病因遺伝子の探索	新堀哲也、井泉瑠美子、西山亜由美、矢尾板全子、大場大樹、守谷充司、井上晋一、舟山亮、城田松之、中山啓子、松原洋一、青木洋子	第3回生命医薬情報学連合大会(仙台)	2014/10/2-4	国内

2. 学会誌・雑誌等における論文掲載

掲載した論文(発表題目)	発表者氏名	発表した場所 (学会誌・雑誌 等名)	発表した時 期	国内・ 外の別
Bilateral giant coronary aneurysms in a 40-year-old male with Noonan syndrome caused by a KRAS germline mutation.	Fujimoto N, Nakajima H, Sugiura E, Dohi K, Kanemitsu S, Yamada N, Aoki Y, Nakatani K, Shimpo H, Nobori T, Ito M.	Int J Cardiol.	173(3):e63-6, 2014	国外
Activating mutations in RRAS underlie a phenotype within the RASopathy spectrum and contribute to leukaemogenesis.	Flex E, Jaiswal M, Pantaleoni F, Martinelli S, Strullu M, Fansa EK, Caye A, De Luca A, Lepri F, Dvorsky R, Pannone L, Paolacci S, Zhang SC, Fodale V, Bocchinfuso G, Rossi C, Burkitt-Wright EM, Farrotti A, Stellacci E, Cecchetti S, Ferese R, Bottero L, Castro S, Fenneteau O, Brethon B, Sanchez M, Roberts AE, Yntema HG, van der Burgt I, Cianci P, Bondeson ML, Digilio MC, Zampino G, Kerr B, Aoki Y, Loh ML, Palleschi A, Di Schiavi E, Carè A, Selicorni A, Dallapiccola B, Cirstea IC, Stella L, Zenker M, Gelb BD, Cavé H, Ahmadian MR, Tartaglia M.	Hum Mol Genet.	23:4315-27, 2014	国外
New BRAF knock-in mice provide a pathogenetic mechanism of developmental defects and a therapeutic approach in cardio-facio-cutaneous syndrome.	Inoue SI, Moriya M, Watanabe Y, Miyagawa-Tomita S, Niihori T, Oba D, Ono M, Kure S, Ogura T, Matsubara Y, Aoki Y.	Hum Mol Genet.	23:6553-66, 2014	国外
Identification of acquired mutations by whole-genome sequencing in GATA-2 deficiency evolving into myelodysplasia and acute leukemia	Fujiwara T, Fukuhara N, Funayama R, Nariai N, Kamata M, Nagashima T, Kojima K, Onishi Y, Sasahara Y, Ishizawa K, Nagasaki M, Nakayama K, Harigae H	Ann Hematol	2014/04	国外
HCV infection enhances Th17 commitment, which could affect the pathogenesis of autoimmune diseases	Kondo Y, Ninomiya M, Kimura O, Machida K, Funayama R, Nagashima T, Kobayashi K, Kakazu E, Kato T, Nakayama K, Lai M. M, Shimosegawa T	PLoS One	2014/06	国外
GNE myopathy associated with congenital thrombocytopenia: A report of two siblings	Izum, R, Niihori T, Suzuki N, Sasahara Y, Rikiishi T, Nishiyama A, Nishiyama S, Endo K, Kato M, Warita H, Konno H, Takahashi T, Tateyama M, Nagashima T, Funayama R, Nakayama K, Kure S, Matsubara Y, Aoki Y, Aoki M	Neuromuscul Disord	2014/12	国外
CRL4(VprBP) E3 Ligase Promotes Monoubiquitylation and Chromatin Binding of TET Dioxygenases.	Nakagawa T, Lv L, Nakagawa M, Yu Y, Yu C, D'Alessio A. C, Nakayama K, Fan H. Y, Chen X, Xiong Y.	Mol Cell	2015/01	国外

舞踏運動を呈したdysferlin異常症の1例.	高橋俊明、今井尚志、田中洋康、吉岡勝、今野秀彦、日向野修一、小野寺好明、齋藤博、木村格、糸山泰人、武田篤、青木正志	JMDD(運動障害)	2014	国内
Targeted next-Generation sequencing effectively analyzed the cystic fibrosis transmembrane conductance regulator gene in pancreatitis.	Nakano E, Masamune A, Niihori T, Kume K, Hamada S, Aoki Y, Matsubara Y, Shimosegawa T.	Dig Dis Sci.	2014/12/10	国外
Variants in the interferon regulatory factor-2 gene are not associated with pancreatitis in Japan.	Nakano E, Masamune A, Kume K, Kakuta Y, Shimosegawa T.	Pancreas.	2014;43:1125-1126.	国外
A novel heterozygous MAP2K1 mutation in a patient with Noonan syndrome with multiple lentigines.	Nishi E, Mizuno S, Nanjo Y, Niihori T, Fukushima Y, Matsubara Y, Aoki Y, Kosho T	Am J Med Genet A.	167(2):407-11, 2015	国外

機関名 慶應義塾大学

2. 学会誌・雑誌等における論文掲載

掲載した論文(発表題目)	発表者氏名	発表した場所(学会誌・雑誌等名)	発表した時期	国内・外の別
Severe craniosynostosis with Noonan syndrome phenotype associated with SHOC2 mutation: clinical evidence of crosslink between FGFR and RAS signaling pathways.	Takenouchi T, Sakamoto Y, Miwa T, Torii C, Kosaki R, Kishi K, Takahashi T, Kosaki K	Am J Med Genet A.	2014 Nov	海外
Porencephaly in a fetus and HANAC in her father: variable expression of COL4A1 mutation.	Takenouchi T, Ohyagi M, Torii C, Kosaki R, Takahashi T, Kosaki K.	Am J Med Genet A	2015 Jan	海外
Paramagnetic Signals in the Globus Pallidus as Late Radiographic Sign of Juvenile-Onset GM1 Gangliosidosis.	Takenouchi T, Kosaki R, Nakabayashi K, Hata K, Takahashi T, Kosaki K.	Pediatr Neurol	2015 Feb	海外
Novel Overgrowth Syndrome Phenotype Due to Recurrent De Novo PDGFRB Mutation.	Takenouchi T, Yamaguchi Y, Tanikawa A, Kosaki R, Okano H, Kosaki K.	J Pediatr	2015 Feb	海外

機関名 (公財)かずさDNA研究所

1. 学会等における口頭・ポスター発表

発表した成果(発表題目、口頭・ポスター発表の別)	発表者氏名	発表した場所(学会等名)	発表した時期	国内・外の別
Implementation of High-Volume Genomic Analyses by Microfluidics/microchip Technologies: Towards Integrative Medical Sciences for Preventive Medicine (口頭発表)	小原 収	ICEP2014、富山	2014/4/24	国内 (国際学会)
What is "Next-Generation DNA Sequencing" for? (口頭発表)	小原 収	熊本大学最先端研究セミナー(リエゾンラボ研究会)	2014/5/7	国内
ヒト遺伝性疾患の構造バイオインフォマティクス (口頭発表)	土方敦、小原収	第86回日本遺伝学学会	2014/9/19	国内
Aicardi-Goutières syndrome is caused by IFIH1 mutations (ポスター発表)	Oda H, Nakagawa K, Abe J, Awaya T, Funabiki M, Hijikata A, Nishikomori R, Funatsuka M, Ohshima Y, Sugawara Y, Yasumi T, Kato H, Shirai T, Ohara O, Fujita T, Heike T	The 64th Annual Meeting of the American Society of Human Genetics (San Diego, CA USA)	2014/10/19	国外
臨床研究のための疾患遺伝子解析パイプラインの構築(口頭発表)	小原 収	第56回日本人類遺伝学会	2014/11/20	国内
IFIH1遺伝子変異はAicardi-Goutières症候群の原因となる(ポスター発表)	小田紘嗣 中川権史 阿部純也 粟屋智就 船曳正英 土方敦 八角高裕 白井剛 小原収 加藤博己 藤田尚志 西小森隆太 平家俊男	第56回日本人類遺伝学会	2014/11/22	国内
次世代シーケンサー(MiSeq)を用いた原発性免疫不全症の遺伝子解析(口頭発表)	中山学、小田紘嗣、八角高裕、西小森隆太、平家俊男、小原収	第8回日本免疫不全症研究会学術集会	2015/1/24	国内
次世代シーケンサーを用いた原発性免疫不全症の迅速遺伝子診断法の確立(口頭発表)	加藤環、釜江智佳子、野々山恵章、今井耕輔、小原収	第8回日本免疫不全症研究会学術集会	2015/1/24	国内

2. 学会誌・雑誌等における論文掲載

掲載した論文(発表題目)	発表者氏名	発表した場所(学会誌・雑誌等名)	発表した時期	国内・外の別
X-Linked Agammaglobulinemia Associated with B-Precursor Acute Lymphoblastic Leukemia.	Hoshino A, Okuno Y, Migita M, Ban H, Yang X, Kiyokawa N, Adachi Y, Kojima S, Ohara O, Kanegane H.	J Clin Immunol. 2015 Jan 16. [Epub ahead of print]	2015, Jan 16	国外

Aicardi-Goutières syndrome is caused by IFIH1 mutations.	Oda H, Nakagawa K, Abe J, Awaya T, Funabiki M, Hijikata A, Nishikomori R, Funatsuka M, Ohshima Y, Sugawara Y, Yasumi T, Kato H, Shirai T, Ohara O, Fujita T, Heike T.	Am J Hum Genet. 2014 Jul 3;95(1):121-5.	2014, July	国外
A complement factor B mutation in a large kindred with atypical hemolytic uremic syndrome.	Funato M, Uemura O, Ushijima K, Ohnishi H, Orii K, Kato Z, Yamakawa S, Nagai T, Ohara O, Kaneko H, Kondo N.	J Clin Immunol. 2014 Aug;34(6):691-5.	2014, Aug	国外
Clinical and genetic characterization of Japanese sporadic cases of periodic Fever, aphthous stomatitis, pharyngitis and adenitis syndrome from a single medical center in Japan.	Kubota K, Ohnishi H, Teramoto T, Kawamoto N, Kasahara K, Ohara O, Kondo N.	J Clin Immunol. 2014 Jul;34(5):584-93.	2014, July	国外
Somatic NLRP3 mosaicism in Muckle-Wells syndrome. A genetic mechanism shared by different phenotypes of cryopyrin-associated periodic syndromes.	Nakagawa K, Gonzalez-Roca E, Souto A, Kawai T, Umebayashi H, Campistol JM, Cañellas J, Takei S, Kobayashi N, Callejas-Rubio JL, Ortego-Centeno N, Ruiz-Ortiz E, Rius F, Anton J, Iglesias E, Jimenez-Treviño S, Vargas C, Fernandez-Martin J, Calvo I, Hernández-Rodríguez J, Mendez M, Dordal MT, Basagaña M, Bujan S, Yashiro M, Kubota T, Koike R, Akuta N, Shimoyama K, Iwata N, Saito MK, Ohara O, Kambe N, Yasumi T, Izawa K, Kawai T, Heike T, Yagüe J, Nishikomori R, Aróstegui JI.	Ann Rheum Dis. 2015 Mar;74(3):603-10.	2015, March	国外
Merkel Cell Polyomavirus-positive Merkel Cell Carcinoma in a Patient with Epidermodysplasia Verruciformis.	Mizuno Y, Kato G, Shu E, Ohnishi H, Fukao T, Ohara O, Fukumoto H, Katano H, Seishima M.	Acta Derm Venereol. 2015 Jan 15;95(1):98-99.	2015, Jan	国外

機関名 浜松医科大学

2. 学会誌・雑誌等における論文掲載

掲載した論文(発表題目)	発表者氏名	発表した場所(学会誌・雑誌等名)	発表した時期	国内・外の別
Compound heterozygous deletions in pseudoautosomal region 1 in an infant with mild manifestations of Langer mesomelic dysplasia.	Tsuchiya T, Shibata M, Numabe H, Jinno T, Nakabayashi K, Nishimura G, Nagai T, Ogata T, Fukami M*:	<i>Am J Med Genet A</i>	2014	国外
Prenatal Genetic testing for a microdeletion at chromosome 14q32.2 imprinted region leading to upd(14)pat-like phenotype.	Sasaki A, Sumie M, Eada S, Kosaki R, Kurosawa K, Fukami M, Sago H, Ogata T, Kagami M*:	<i>Am J Med Genet A</i>	2014	国外

IMAGe syndrome: clinical and genetic implications based on Investigations in three Japanese patients.	Kato F, Hamajima T, Hasegawa T, Amano N, Horikawa R, Nishimura G, Nakashima S, Fuke T, Sano S, Fukami M, Ogata T*:	<i>Clin Endocrinol</i>	2014	国外
Genome-wide parent-of-origin DNA methylation analysis reveals the intricacies of the human imprintome and suggests a germline methylation independent establishment of imprinting.	Court F, Tayama C, Romanelli V, Martin-Trujillo A, Iglesias-Platas I, Okamura K, Sugahara N, Simon C, Moore H, Harness J, Keirstead H, Vicente Sanchez-Mut J, Kaneki E, Lapunzina P, Soejima H, Wake N, Esteller M, Ogata T, Hata K, Nakabayashi K, Monk D*:	<i>Genome Res</i>	2014	国外
<i>TBX1</i> mutation identified by exome sequencing in a Japanese family with 22q11.2 deletion syndrome-like craniofacial features and hypocalcemia.	Ogata T*, Niihori T, Tanaka N, Kawai M, Nagashima T, Funayama R, Nakayama K, Nakashim S, Kato F, Fukami M, Aoki Y, Matsubara Y:	<i>PLoS One</i>	2014	国外
A novel <i>de novo</i> point mutation of OCT-binding site in the <i>IGF2/H19</i> -imprinting control region in a patient with Beckwith-Wiedemann syndrome patient.	Higashimoto K, Jozaki K, Kosho T, Matsubara K, Sato T, Yamada D, Yatsuki H, Maeda T, Ohtsuka Y, Nishioka K, Joh K, Koseki H, Ogata T, SoejimaH*:	<i>Clin Genet</i>	2014	国外
Comprehensive and quantitative multilocus methylation analysis reveals the susceptibility of specific imprinted differentially methylated regions (DMRs) to aberrant methylation in Beckwith-Wiedemann syndrome with epimutations.	Maeda T, Higashimoto K, Jozaki K, Hitomi H, Nakabayashi K, Makita Y, Tonoki H, Okamoto N, Takada F, Ohashi H, Migita M, Kosaki R, Matsubara K, Ogata T, Matsuo M, Hamasaki Y, Ohtsuka Y, Nishioka K, Joh K, Mukai T, Hata K, Soejima H*:	<i>Genet Med</i>	2014	国外
Japanese founder duplications/triplications involving <i>BHLHA9</i> are associated with split-hand/foot malformation with or without long bone deficiency and Gallop-Wolfgang complex.	Nagata E, Kano H, Kato F, Yamaguchi R, Nakashima S, Takayams S, Kosaki R, Tonoki H, Mizuno S, Watanabe S, Yoshiura K, Kosho T, Hasegawa T, Kimizuka M, Suzuki A, Shimizu K, Ohashi H, Haga N, Numabe H, Horii E, Nagai T, Yoshihashi H, Nishimura G, Toda T, Takada S, Yokoyama S, Asahara H, Sano S, Fukami M, Ikegawa S, Ogata T*:	<i>Orphanet J Rare Dis</i>	2014	国外
Epimutations of the IG-DMR and the <i>MEG3</i> -DMR at the 14q32.2 imprinted region in two patients with Silver-Russell syndrome-compatible phenotype.	Kagami M, Mizuno S, Matsubars K, Nakabayashi K, Sano S, Fuke T, Fukami M, Ogata T*:	<i>Eur J Hum Genet</i>	in press	国外
Silver-Russell syndrome without body asymmetry in three patients with duplications of maternally derived chromosome 11p15 involving <i>CDKN1C</i> .	Nakashima S, Kato F, Kosho T, Nagasaki K, Kikuchi T, Kagami M, Fukami M, Ogata T*:	<i>J Hum Genet</i>	in press	国外

Comprehensive clinical studies in 34 patients with molecularly defined UPD(14)pat and related conditions (Kagami-Ogata syndrome).	Kagami M, Kurosawa K, Miyazaki O, Ishino F, Matsuoka K, Ogata T*:	<i>Eur J Hum Genet</i>	in press	国外
---	---	------------------------	----------	----

機関名 藤田保健衛生大学

1. 学会等における口頭・ポスター発表

発表した成果(発表題目、口頭・ポスター発表の別)	発表者氏名	発表した場所(学会等名)	発表した時期	国内・外の別
Age-related decrease of meiotic cohesins in human oocytes.	Kurahashi H, Tsutsumi M, Fujiwara R, Nishizawa H, Kogo H, Inagaki H, Ohye T, Kato T, Fujii T.	Eshre 2014. Munich, Germany.	June 29- July 2, 2014.	国外
Obstetric complication-associated ANXA5 promoter polymorphisms affect gene expression via G-quadruplex structure in vivo.	Inagaki H, Ota S, Nishizawa H, Miyamura H, Nakahira K, Suzuki M, Tsutsumi M, Kato T, Nishiyama S, Udagawa Y, Yanagihara I, Kurahashi H.	FASEB SRC, Dynamic DNA Structures in Biology, Itasca, Illinois.	July 20 - 25, 2014.	国外
Detection of in vivo G-quadruplex structure of the ANXA5 promoter that contributes to the recurrent pregnancy loss.	Inagaki H, Ota S, Miyamura H, Tsutsumi M, Kato T, Nishizawa H, Yanagihara I, Kurahashi H.	ASHG 2014, San Diego, CA.	October 18-22, 2014.	国外
Two cases of lissencephaly with marked hydrocephalus caused by TUBA1A mutation.	Ishihara N, Yokoi S, Yamamoto H, Natsume J, Tsutsumi M, Ohye T, Kato M, Saito S, Kurahashi H.	ASHG 2014, San Diego, CA.	October 18-22, 2014.	国外
EFNB1 mutation found in patients with craniofrontonasal syndrome in a Japanese family.	Kato H, Okumoto T, Yoshimura Y, Taguchi Y, Sugimoto M, Inagaki H, Kurahashi H.	The 10th Asian Pacific Craniofacial Association Conference, Adelaide, South Australia.	October 3 - 5, 2014.	国外
Cytogenetic analysis of monopronucleated (1PN) zygotes after intracytoplasmic sperm injection and conventional in-vitro fertilization.	Nishiyama S, Kato T, Kani C, Miyazaki J, Nishizawa H, Ochi M, Fujii T, Kurahashi H.	International Society for Mild Approaches in Assisted Reproduction. Sydney, Australia.	Sep 10-12. 2014.	国外

2. 学会誌・雑誌等における論文掲載

掲載した論文(発表題目)	発表者氏名	発表した場所(学会誌・雑誌等名)	発表した時期	国内・外の別
Age-related decrease of meiotic cohesins in human oocytes.	Tsutsumi M, Fujiwara R, Nishizawa H, Ito M, Kogo H, Inagaki H, Ohye T, Kato T, Fujii T, Kurahashi H.	PLoS One 2014: 9(5): e96710.	2014	国外

Dual roles for the telomeric repeats in chromosomally integrated human herpesvirus-6.	Ohye T, Inagaki H, Ihira M, Higashimoto Y, Kato K, Oikawa J, Yagasaki H, Niizuma T, Takahashi Y, Kojima S, Yoshikawa T, Kurahashi H.	Sci Rep 2014: 4: 4559.	2014	国外
Breakpoint analysis of the recurrent constitutional t(8;22)(q24.13;q11.21) translocation.	Mishra D, Kato T, Inagaki H, Kosho T, Wakui K, Kido Y, Sakazume S, Taniguchi-Ikeda M, Morisada N, Iijima K, Fukushima Y, Emanuel BS, Kurahashi H.	Mol Cytogenet 2014: 7: 55.	2014	国外
Signature of backward replication slippage at the copy number variation junction.	Ohye T, Inagaki H, Ozaki M, Ikeda T, Kurahashi H.	J Hum Genet 2014: 59(5): 247-250.	2014	国外
Analysis of the t(3;8) of hereditary renal cell carcinoma: A palindrome mediated translocation.	Kato T, Franconi CP, Sheridan MB, Hacker AM, Inagakai H, Glover TW, Arlt MF, Drabkin HA, Gemmill RM, Kurahashi H, Emanuel BS.	Cancer Genet 2014: 207(4): 133-140.	2014	国外

機関名 富山大学

2. 学会誌・雑誌等における論文掲載

掲載した論文(発表題目)	発表者氏名	発表した場所 (学会誌・雑誌 等名)	発表した時期	国内・ 外の別
Accurate prediction for the stage of histological chorioamnionitis before delivery by amniotic fluid IL-8 level.	Yoneda S, Shiozaki A, Ito M, Yoneda N, Inada K, Yonezawa R, Kigawa M, Saito S.	Am J Reprod Immunol.	in press	国外
Prenatal diagnosis of enterolithiasis at 18 weeks: multiple foci of intraluminal calcified meconium within echogenic bowel.	Shiozaki A, Yoneda S, Iizuka T, Kusabiraki T, Ito M, Yoneda N, Yoshimoto H, Saito S.	J Med Ultrasonics. 42:113-116	2015	国外
Helios-positive functional regulatory T cells are decreased in decidua of miscarriage cases with normal fetal chromosomal content.	Inada K, Shima T, Ito M, Ushijima A, Saito S.	J Reprod Immunol. 107:10-19	2015	国外
Intestinal microbiota is different in women with preterm birth: Results from terminal restriction fragment length polymorphism analysis.	Shiozaki A, Yoneda S, Yoneda N, Yonezawa R, Matsubayashi T, Seo G, Saito S.	PLoS ONE. 9(11):e111374	2014	国外
Extensive serum biomarker analysis in patients with enterohemorrhagic Escherichia coli O111-induced hemolytic-uremic syndrome.	Shimizu M, Kuroda M, Inoue N, Konishi M, Igarashi N, Taneichi H, Kanegane H, Ito M, Saito S, Yachie A.	Cytokine. 66:1-6	2014	国外

Whole exome sequencing revealed biallelic IFT122 mutations in a family with CED1 and recurrent pregnancy loss.	Tsurusaki Y, Yonezawa R, Furuya M, Nishimura G, Pooh RK, Nakashima M, Saitu H, Miyake N, Saito S, Matsumoto N.	Clin Genet 85:592-594	2014	国外
Multiple pregnancy, short cervix, part-time worker, steroid use, low educational level, and male fetus are risk factors for preterm birth in Japan: A multicenter, prospective study.	Shiozaki A, Yoneda S, Nakabayashi M, Takeda Y, Takeda S, Sugimura M, Yoshida K, Tajima A, Manabe M, Akagi K, Nakagawa S, Tada K, Imafuku N, Ogawa M, Mizunoe T, Kanayama N, Itoh H, Minoura S, Ogino M, Saito S.	J Obstet Gynaecol Res 40: 53-61.	2014	国外

(注1) 発表者氏名は、連名による発表の場合には、筆頭者を先頭にして全員を記載すること。

(注2) 本様式はexcel形式にて作成し、甲が求める場合は別途電子データを納入すること。

IV. 研究成果の刊行物・別刷

New *BRAF* knockin mice provide a pathogenetic mechanism of developmental defects and a therapeutic approach in cardio-facio-cutaneous syndrome

Shin-ichi Inoue¹, Mitsuji Moriya¹, Yusuke Watanabe⁴, Sachiko Miyagawa-Tomita^{5,6}, Tetsuya Niihori¹, Daiju Oba¹, Masao Ono², Shigeo Kure³, Toshihiko Ogura⁴, Yoichi Matsubara^{1,7} and Yoko Aoki^{1,*}

¹Department of Medical Genetics, ²Department of Pathology, ³Department of Pediatrics, Tohoku University School of Medicine, Sendai, Japan, ⁴Department of Developmental Neurobiology, Institute of Development, Aging and Cancer, Tohoku University, Sendai, Japan, ⁵Department of Pediatric Cardiology, ⁶Division of Cardiovascular Development and Differentiation, Medical Research Institute, Tokyo Women's Medical University, Tokyo, Japan and ⁷National Research Institute for Child Health and Development, Tokyo, Japan

Received March 15, 2014; Revised and Accepted July 14, 2014

Cardio-facio-cutaneous (CFC) syndrome is one of the 'RASopathies', a group of phenotypically overlapping syndromes caused by germline mutations that encode components of the RAS–MAPK pathway. Germline mutations in *BRAF* cause CFC syndrome, which is characterized by heart defects, distinctive facial features and ectodermal abnormalities. To define the pathogenesis and to develop a potential therapeutic approach in CFC syndrome, we here generated new knockin mice (here *Braf*^{Q241R/+}) expressing the *Braf* Q241R mutation, which corresponds to the most frequent mutation in CFC syndrome, Q257R. *Braf*^{Q241R/+} mice manifested embryonic/neonatal lethality, showing liver necrosis, edema and craniofacial abnormalities. Histological analysis revealed multiple heart defects, including cardiomegaly, enlarged cardiac valves, ventricular noncompaction and ventricular septal defects. *Braf*^{Q241R/+} embryos also showed massively distended jugular lymphatic sacs and subcutaneous lymphatic vessels, demonstrating lymphatic defects in RASopathy knockin mice for the first time. Prenatal treatment with a MEK inhibitor, PD0325901, rescued the embryonic lethality with amelioration of craniofacial abnormalities and edema in *Braf*^{Q241R/+} embryos. Unexpectedly, one surviving pup was obtained after treatment with a histone 3 demethylase inhibitor, GSK-J4, or NCDM-32b. Combination treatment with PD0325901 and GSK-J4 further increased the rescue from embryonic lethality, ameliorating enlarged cardiac valves. These results suggest that our new *Braf* knockin mice recapitulate major features of RASopathies and that epigenetic modulation as well as the inhibition of the ERK pathway will be a potential therapeutic strategy for the treatment of CFC syndrome.

INTRODUCTION

Cardio-facio-cutaneous (CFC) syndrome is an autosomal dominant congenital anomaly syndrome, characterized by a distinctive facial appearance, short stature, congenital heart defects, intellectual disability and ectodermal abnormalities such as

sparse, fragile hair, hyperkeratotic skin lesions and a severe generalized ichthyosis-like condition (1). The cardiac defects observed in CFC syndrome include pulmonary valve stenosis, hypertrophic cardiomyopathy and atrial septal defects. Increased nuchal translucency/fatal cystic hygroma colli due to lymphatic defects is also occasionally observed in affected individuals (2).

*To whom correspondence should be addressed at: Department of Medical Genetics, Tohoku University School of Medicine, 1-1 Seiryō-machi, Aoba-ku, Sendai 980-8574, Japan. Tel: +81 227178139; Fax: +81 227178142; Email: aokiy@med.tohoku.ac.jp

Our group as well as another group has identified germline *BRAF* mutations in 50–75% of patients with CFC syndrome (3–6). Other known CFC-causative genes include *KRAS* as well as *MAP2K1* and *MAP2K2* (MEK1 and MEK2, respectively) (3–6), all located in the same RAS–MAPK pathway that regulates cell differentiation, proliferation, survival and apoptosis (7). Germline mutations associated with RAS–MAPK pathway components cause partially overlapping disorders, including Noonan syndrome, Costello syndrome, LEOPARD syndrome, neurofibromatosis type 1 and Legius syndrome (neurofibromatosis type 1-like syndrome). These syndromes are now collectively termed RASopathies or RAS–MAPK syndromes (8–10).

BRAF is a serine threonine kinase which regulates the RAS–MAPK signaling pathway. Somatic *BRAF* mutations have been identified in 7% of human tumors, including melanoma, papillary thyroid carcinoma, colon cancer and ovarian cancer (11). The *BRAF* V600E mutation, located in the catalytic kinase domain (conserved region (CR) 3 domain), accounts for 90% of all somatic *BRAF* mutations. In contrast, *BRAF* V600E mutation has not been identified in CFC syndrome. Germline *BRAF* mutations in CR3 kinase domain, including G464R, G469E and L597V, were overlapping those in somatic mutations (4,5,12,13). In contrast, germline mutations in the CR1 domain have been rarely identified in somatic cancers. The most frequent mutations identified in CFC syndrome patients are substitutions of the residue Gln257 (p.Q257R and p.Q257K) in the CR1 domain, which account for ~40% (13). Previous studies have shown that the activation of downstream signaling, including ELK transactivation, is weaker in cells expressing the Q257R mutation than in those expressing V600E (3).

Braf is ubiquitously expressed in murine organs at mid-gestation, and high levels of its expression are found in the brain and testes at adult stage (14,15). *Braf* knockout mice have been found to die at mid-gestation from vascular defects due to enlarged blood vessels and apoptotic death of differentiated endothelial cells (16). Heterozygous knockin mice constitutively expressing V600E mutation have been found to exhibit embryonic lethality (17). Knockin mice expressing a hypomorphic *BRAF* V600E allele have been reported to show phenotypes partially overlapping those of CFC syndrome patients, including small size, craniofacial abnormalities and epileptic seizures (18). However, no mouse model for CFC syndrome expressing a *Braf* mutation in the CR1 domain has been generated and no therapeutic approach has been developed. In the present study, we generated knockin mice expressing CFC syndrome-associated *Braf* Q241R mutation, corresponding to *BRAF* Q257R mutation, in order to investigate the molecular pathogenesis and potential therapeutic possibilities for CFC syndrome.

RESULTS

Generation of a CFC syndrome mouse model

We have previously reported that the transcriptional activity of ELK, downstream of ERK, was enhanced by the transient over-expression of human *BRAF* Q257R in NIH3T3 cells (3). To verify whether the expression of mouse *Braf* Q241R enhances ELK transcription as *BRAF* Q257R, reporter assays were performed in NIH3T3 cells. The expression of *Braf* Q241R and

that of V637E, which corresponds to *BRAF* V600E, were ~2.7- and 8.4-fold higher than that of *Braf* WT, respectively (Fig. 1A). These results suggest that the *Braf* Q241R mutation is a gain-of-function mutation, although the activation is weaker than that observed in *Braf* V637E.

To investigate the gain-of-function effect of the *Braf* Q241R mutation on development, *Braf* Q241R knockin mice were generated (Fig. 1B). The targeting vector (Fig. 1B) was electroporated into ES cells and targeted clones were identified by Southern blotting (Fig. 1C). Appropriate ES cells were injected into BALB/c blastocysts and chimeras were obtained from six independent ES cell clones (hereafter referred to as *Braf*^{Q241R Neo/+}). To induce ubiquitous expression of *Braf* Q241R in germ cells, the *Braf*^{Q241R Neo/+} mice were crossed with CAG-Cre transgenic mouse (*Braf*^{+/+}; *Cre*) and genotyping was confirmed by PCR (Supplementary Material, Fig. S1). Furthermore, sequencing was performed to confirm that Cre recombination resulted in *Braf* Q241R expression (Fig. 1D).

To examine if cell signaling pathways, including ERK, JNK, p38 and PI3K–AKT pathways, were altered in *Braf*^{Q241R/+}; *Cre* embryos, western blotting analysis was performed using cell extracts derived from whole-mouse embryos and brain. Protein levels of BRAF, CRAF, phosphorylated MEK and ERK in *Braf*^{Q241R/+}; *Cre* whole embryos were similar to those of *Braf*^{+/+}; *Cre* (Fig. 1E; Supplementary Material, Table S1), whereas phosphorylated MEK protein levels were higher in the brain of *Braf*^{Q241R/+}; *Cre* embryos (Fig. 1F; Supplementary Material, Table S2). Unexpectedly, phosphorylated p38 and AKT (Thr308) protein levels were somewhat lower in *Braf*^{Q241R/+}; *Cre* whole embryos at embryonic day (E) 14.5 (Fig. 1E; Supplementary Material, Table S1). These results suggest that *Braf*^{Q241R/+}; *Cre* embryos at E14.5 show a decrease of phosphorylated p38 and AKT (Thr308) protein levels.

Germline expression of *Braf* Q241R results in embryonic/neonatal lethality

Genotype analysis of embryos from an intercross between *Braf*^{+/+}; *Cre* and *Braf*^{Q241R Neo/+} mice showed no surviving *Braf*^{Q241R/+}; *Cre* littermates at weaning, whereas *Braf*^{+/+}; *Braf*^{+/+}; *Cre* and *Braf*^{Q241R Neo/+} littermates survived (Table 1). A normal Mendelian ratio was observed by E14.5. However, the survival rate of *Braf*^{Q241R/+}; *Cre* embryos dropped after E16.5. At E16.5, ~9.8% of embryos (4 of 41) were grossly hemorrhagic and edematous such as nuchal translucency (Fig. 2A, Table 1). Other *Braf*^{Q241R/+}; *Cre* embryos appeared normal (Fig. 2B) with no difference in body weight (data not shown). *Braf*^{Q241R/+}; *Cre* embryos, which were delivered by cesarean section at E18.5 and E19.5, remained pale and without movement or gasped for breath with cyanotic appearance, resulting in death within a few hours. A few embryos showed mandibular hypoplasia (2 of 39, 5.1%) and kyphosis (Fig. 2C and D).

Gross observation showed increased heart size in *Braf*^{Q241R/+}; *Cre* embryos at E16.5. At E18.5, *Braf*^{Q241R/+}; *Cre* embryos revealed severe peripheral liver necrosis (15 of 17, 88%) with decreased liver size and liver weight (Fig. 2E; Supplementary Material, Fig. S2). At E16.5, decreased liver weight was already observed (data not shown), although the gross appearance of the liver appeared normal. To examine if delayed lung maturation causes neonatal lethality, the histology of lung in

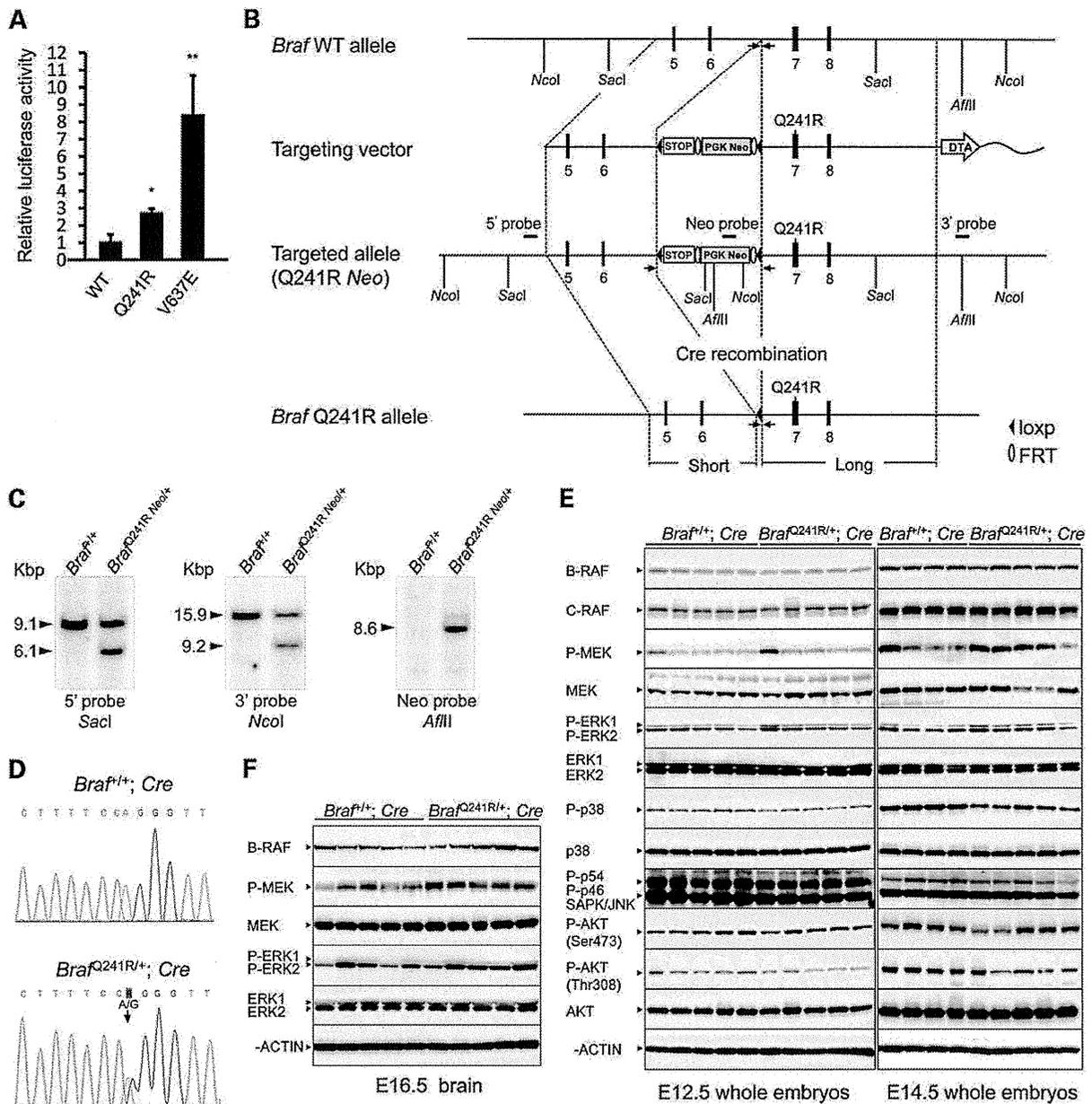


Figure 1. Generation of *Braf* Q241R knockin mice. (A) NIH 3T3 cells were transfected with the ELK1-GAL4 vector, the GAL4-luciferase trans-reporter vector, pRLnull-luc control vector and each mouse *Braf* expression plasmid, and reporter activities were determined as described in Materials and Methods. Luciferase activities were normalized with pRLnull-luc activities, containing distinguishable *R. reniformis* luciferase. Data are the means \pm SD ($n = 4$). p.V637E in mouse *Braf* corresponds to oncogenic p.V600E in human *BRAF*. *, $P < 0.05$, **, $P < 0.01$ versus WT. WT, wild type. (B) Exons (solid boxes), PGK-Neomycin (PGK-Neo) cassette (gray box), STOP transcriptional sequences (open box), loxp sites (arrowheads) and Fip recombination target sites (ellipses) are indicated. Cleavage sites for diagnostic enzymes (*SacI*, *NcoI* and *AflIII*) and the probes (5'-, 3'- and Neo probe) used to identify the homologous recombination are indicated. The PGK-Neo cassette was removed by crossing with CAG-Cre transgenic mice (*Braf*^{+/+}; Cre). The arrow indicates the positions of PCR primers used for genotyping of positive ES cells and mice. p. Q241R in mouse *Braf* corresponds to p.Q257R in human *BRAF*. DTA, diphtheria toxin A. (C) Southern blotting of ES cell clones. Genomic DNA from *Braf*^{+/+} and *Braf*^{Q241R Neo/+} ES cells was digested with *SacI* (5' probe), *NcoI* (3' probe) or *AflIII* (Neo probe) and subjected to Southern blotting with a 5', 3' or Neo probe. The 5', 3' or Neo probe detects the 9.1-kb (*Braf* WT) and 6.1-kb (*Braf*^{Q241R Neo/+}) *SacI* fragments, the 15.9 kb (*Braf* WT) and 9.2 kb (*Braf*^{Q241R Neo/+}) *NcoI* fragments or the 8.6 kb (*Braf*^{Q241R Neo/+}) *AflIII* fragment, respectively. (D) RNA was isolated from the brain of *Braf*^{+/+}; Cre and *Braf*^{Q241R/+}; Cre embryos at E18.5, and reverse transcribed into cDNA. Sanger sequencing was carried out using the cDNA. The arrow indicates the Q241R mutation in *Braf* exon 7. (E and F) Protein extracts from whole-mouse embryos (E12.5 and E14.5) and brain (E16.5) ($n = 4-5$ of each genotype) were subjected to western blotting with the indicated antibodies. β -Actin is shown as a loading control. The arrowheads indicate the bands corresponding to each protein.

Table 1. Genotyping of pups resulting from intercross between *Braf*^{+/+}; *Cre* and *Braf*^{Q241R} *Neol*^{+/+} mice

Age	<i>Braf</i> ^{+/+}	<i>Braf</i> ^{+/+} ; <i>Cre</i>	<i>Braf</i> ^{Q241R} <i>Neol</i> ^{+/+}	<i>Braf</i> ^{Q241R/+} ; <i>Cre</i>	<i>n</i>	<i>P</i>
E12.5	24	29	23	23	99	0.80
E13.5	5	14	6	6 (2 [1])	31	0.08
E14.5	19	22 (1)	23	11 (1 [1])	75	0.19
E16.5	57	60	55	34 (7 [4])	206	0.04
E18.5	16	23	20	0 (17 [4])	59	<0.0001
E19.5	11	16	11	0 (11 [1])	38	<0.01
Weaning (P21)	56	54	56	0	166	<0.0001
Expected	25%	25%	25%	25%		

Deviation from the expected Mendelian ratios was assessed by the χ^2 test. The number of dead embryos is shown in parentheses. The number of edematous embryos is shown in brackets. P: postnatal day.

Braf^{Q241R/+}; *Cre* embryos was examined at E18.5 and E19.5. Lungs of the mutant embryos appeared normal and were able to inflate, but ~11.1% of embryos (1 of 9) showed alveolar hemorrhage (Supplementary Material, Fig. S3). Thyroid transcription factor-1 (TTF-1; lung epithelial cells marker), pro-surfactant protein C and PAS staining showed similar levels in *Braf*^{Q241R} *Neol*^{+/+} and *Braf*^{Q241R/+}; *Cre* embryos (Supplementary Material, Fig. S4), suggesting that lung development and maturation are normal. Gross observation suggests that *Braf*^{Q241R/+}; *Cre* embryos show embryonic/neonatal lethality, cardiomegaly, liver necrosis, edema and craniofacial abnormalities.

Braf^{Q241R/+}; *Cre* embryos display various heart defects

Because *Braf*^{Q241R/+}; *Cre* embryos showed cardiomegaly and liver necrosis, possibly due to heart failure (Fig. 2E), detailed histological analysis of the heart at different embryonic stages was conducted. At E12.5, the hearts of *Braf*^{Q241R/+}; *Cre* embryos appeared normal (Supplementary Material, Fig. S5A), but showed an enlarged pulmonary valve and a dramatic increase in the density of trabeculae (hypertrabeculation) at E14.5 (Supplementary Material, Fig. S5B). At E16.5, 13 of 14 (93%) *Braf*^{Q241R/+}; *Cre* embryos (excluding edematous embryos) had various heart defects (Supplementary Material, Tables S3 and S4). Hypertrophy of pulmonary, tricuspid and mitral valves was present in 7, 8 and 9 of 14 embryos, respectively (Fig. 3A; Supplementary Material, Tables S3 and S4). In particular, hypertrophy in pulmonary valve leaflets was prominent, plugging the entire space of the pulmonary valve ring (Fig. 3B). Other heart defects observed in *Braf*^{Q241R/+}; *Cre* embryos included ventricular septal defect (VSD) in 2 of 14 embryos (Fig. 3A), abnormal endocardial cushion in 2 (Fig. 3A), hypertrabeculation in 3 (Fig. 3A), epicardial blisters in 2 (Fig. 3A and C), a thickened trabecular layer and thinned compact layer in the left, right or combined myocardium (noncompaction: one case of cardiomyopathy accompanied by cardiac hypertrophy) in 4 (Fig. 3D) and hypoplasia of the coronary arteries in 3. The ventricular radius and the thickness of the pulmonary and tricuspid valves were significantly higher in *Braf*^{Q241R/+}; *Cre* embryos, suggesting cardiac enlargement and thickened pulmonary and tricuspid valves (Fig. 3E). These results suggest that *Braf*^{Q241R/+}; *Cre* embryos develop various congenital heart defects, which almost certainly contributes to embryonic lethality.

Braf^{Q241R/+}; *Cre* embryo hearts exhibit enhancement of cell proliferation, ERK signaling activation and decrease of phosphorylated p38 and AKT

To examine if heart defects observed in *Braf*^{Q241R/+}; *Cre* embryos are caused by increased cell proliferation and/or reduced cell death, cell proliferation was analyzed by phosphohistone H3 (pHH3) immunostaining and cell death by TUNEL assay. At E13.5, regarding heart abnormalities in each embryo, the number of pHH3-positive-stained cells varied. pHH3-positive-stained cells in the interventricular septum and myocardium increased in *Braf*^{Q241R/+}; *Cre* embryos (Fig. 4A and B). At E16.5, the nucleus of pHH3-positive cells increased in the interventricular septum in embryos with VSD (Fig. 4C). *Braf*^{Q241R/+}; *Cre* embryos had more pHH3-positive cells in pulmonary valves (Fig. 4D). In contrast to cell proliferation, hardly any cells undergoing apoptosis were observed in either *Braf*^{+/+}; *Cre* or *Braf*^{Q241R/+}; *Cre* at E13.5 and E16.5 (data not shown). These results suggest that the cell proliferation state depends on heart abnormalities in each embryo at E16.5 and that the increased staining for pHH3 in the interventricular septum was associated with VSD.

To examine if the cardiac signaling pathways were altered in *Braf*^{Q241R/+}; *Cre* embryos, the activation of kinases was screened in various signaling pathways using a phospho-kinase array followed by western blotting of the lysates from hearts of *Braf*^{Q241R/+}; *Cre* embryos at E16.5 (Fig. 4E and F; Supplementary Material, Fig. S6). No changes in phosphorylated ERK protein levels in both the phospho-kinase array and western blotting were observed. In contrast, phosphorylated p38, AKT (Ser473) and AKT (Thr308) protein levels, which are not direct targets of BRAF, were relatively lower in *Braf*^{Q241R/+}; *Cre* embryos than in *Braf*^{+/+}; *Cre*, which was confirmed by western blotting. To verify the activation of transcription factors downstream of ERK, the expression of ELK1 and the PEA3 (polyoma enhancer activator 3) subfamily Ets transcription factors were examined by quantitative real-time PCR, these expressions being known as transcriptional targets of FGF signaling-mediated activation of ERK in heart and oncogenic BRAF signaling in melanoma (19,20). At E13.5, E16.5 and E18.5, cardiac mRNA levels of *Etv1*, *Etv4* and *Etv5*, but not *Elk1*, were significantly higher in *Braf*^{Q241R/+}; *Cre* embryos than those in *Braf*^{+/+}; *Cre* (Fig. 4G; Supplementary Material, Fig. S7). Next, we investigated the influence of genes responsible for hypertrophic cardiomyopathy and

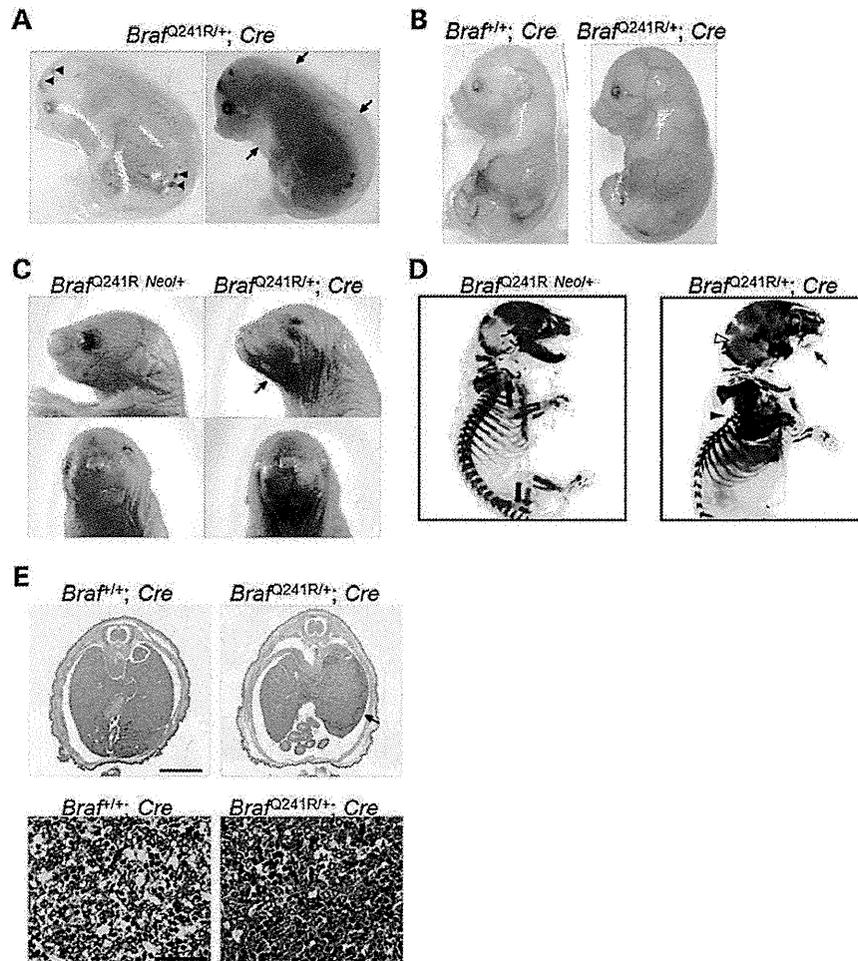


Figure 2. Lethal phenotypes of *Braf*^{Q241R/+}; *Cre* embryos. (A and B) Gross appearance of *Braf*^{+/+}; *Cre* and *Braf*^{Q241R/+}; *Cre* embryos at E16.5. (A) Arrowheads and arrows indicate hemorrhage and edema, respectively. The right panel shows *Braf*^{Q241R/+}; *Cre* embryos with transmitted illumination. (C) Craniofacial structure of *Braf*^{Q241R Neo+/+} and *Braf*^{Q241R/+}; *Cre* embryos at E19.5. The arrow indicates mandibular hypoplasia. (D) Alcian Blue/Alizarin Red staining of *Braf*^{Q241R Neo+/+} and *Braf*^{Q241R/+}; *Cre* embryos at E19.5. The arrow, solid arrowhead and open arrowhead indicate mandibular hypoplasia, kyphosis and ossification in the interparietal bone, respectively. (E) H&E staining of liver sections of *Braf*^{+/+}; *Cre* and *Braf*^{Q241R/+}; *Cre* embryos at E18.5. The arrow indicates hepatic necrosis. The lower panel shows higher magnification views of hepatic necrosis. Scale bars in upper panels = 200 μ m and in lower panels = 50 μ m.

cardiac development in *Braf*^{Q241R/+}; *Cre* embryos at E18.5, which exhibited a cardiomyopathy phenotype, such as cardiac enlargement and noncompaction (Fig. 3D and E) and structural abnormalities, including VSD. No differences in mRNA levels of cardiomyopathy-specific genes (*Myh6* and *Myh7*) and genes related to the heart formation and development (*Gata4* and *Nkx2.5*) were observed (Fig. 4G). These results suggest that ERK activation, including increased mRNA levels of Ets transcription factors, and decreased levels of p38 and AKT exist in heart tissues of *Braf*^{Q241R/+}; *Cre* embryos.

Braf^{Q241R/+}; *Cre* embryos develop lymphangiectasia

Patients with RASopathies, including CFC syndrome and Noonan syndrome, exhibit nuchal translucency, which is subcutaneous fluid collection in the fetal neck visualized by

ultrasonography. Nuchal translucency is caused by distended jugular lymphatic sacs (JLSs), which result from a disturbance in differentiation of lymphatic endothelial cells (21,22). We hypothesized that the hemorrhage and edema in *Braf*^{Q241R/+}; *Cre* embryos may be caused by defective lymphatic development. Histological examination revealed distended and blood-filled JLSs in *Braf*^{Q241R/+}; *Cre* embryos but not in *Braf*^{+/+}; *Cre* embryos at E12.5 and E16.5 (Fig. 5A and B; Supplementary Material, Fig. S8A). The primary lymphatic sacs are remodeled to produce a hierarchically organized network of lymphatic capillaries and collecting lymph vessels at stages between E14.5 and postnatal stages (23). The JLSs are hardly observed in mouse embryos at E16.5. In *Braf*^{Q241R/+}; *Cre* embryos at E16.5, cavities such as the JLSs of mouse embryos from E12.5 to E14.5 were observed (Fig. 5B), suggesting defective lymphatic development from the cardinal vein in *Braf*^{Q241R/+}; *Cre*

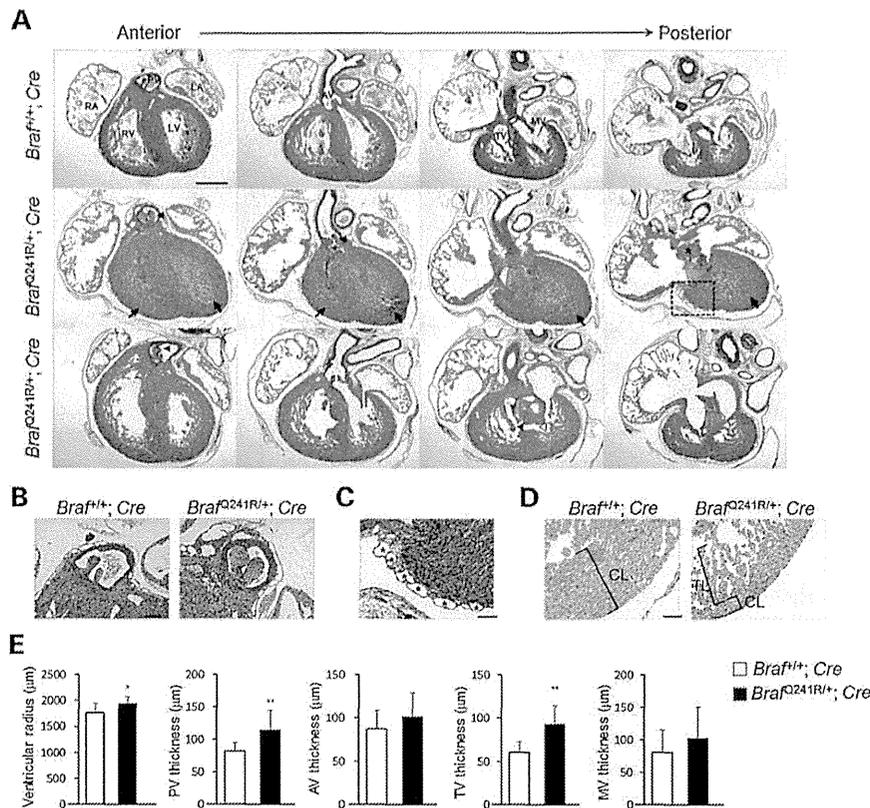


Figure 3. Cardiac phenotype of *Braf*^{Q241R/+}; *Cre* embryos. (A–D) H&E staining of sequential anterior to posterior sections of embryonic hearts from *Braf*^{+/+}; *Cre* and *Braf*^{Q241R/+}; *Cre* at E16.5. A dramatic increase in density of trabeculae (arrows), enlarged valves (solid arrowheads), VSD (open arrowhead) and abnormal endocardial cushion (asterisk) are observed. Scale bars 500 µm (A) and 100 µm (B–D). (B) Higher magnification of the pulmonary valves in *Braf*^{+/+}; *Cre* and *Braf*^{Q241R/+}; *Cre* embryos. (C) Higher magnification of the boxed region in Figure 3A showing the epicardial blisters (asterisks) in *Braf*^{Q241R/+}; *Cre* embryos at E16.5. (D) Representative image of noncompaction in hearts from *Braf*^{Q241R/+}; *Cre* embryos at E16.5. (E) The ventricular radius and the thicknesses of the cardiac valve leaflets were measured at their largest diameter in serial sections of *Braf*^{+/+}; *Cre* and *Braf*^{Q241R/+}; *Cre* embryos at E16.5. Data are the means ± SD (*Braf*^{+/+}; *Cre* (*n* = 9) and *Braf*^{Q241R/+}; *Cre* (*n* = 14)). **P* < 0.05, ***P* < 0.01 versus *Braf*^{+/+}; *Cre*. LV, left ventricle; RV, right ventricle; LA, left atrium; RA, right atrium; PV, pulmonary valve; AV, aortic valve; TV, tricuspid valve; MV, mitral valve; CL, compact layer; TL, trabecular layer.

embryos. To examine the network formation of blood and lymphatic vessels, we performed immunostaining using antibodies against lymphatic vessel endothelial hyaluronan receptor 1 (LYVE-1; lymphatic endothelial cell-specific marker), α -SMA for staining of vessels with smooth muscle and CD31 (platelet-endothelial cell adhesion molecule-1, PECAM-1) for staining of vascular endothelial cells. At E12.5, the cells lining JLSs in both *Braf*^{+/+}; *Cre* and *Braf*^{Q241R/+}; *Cre* embryos were positive for LYVE-1 (Fig. 5C), whereas slightly CD31-positive cells were detected in JLSs and the jugular vein (Fig. 5D). No α -SMA expression was observed (Supplementary Material, Fig. S8B). At E16.5, the cavities such as the JLSs in *Braf*^{Q241R/+}; *Cre* embryos were negative for LYVE-1, α -SMA and CD31 (Fig. 5E; Supplementary Material, Fig. S8C and D), but the subcutaneous lymphatic vessels were markedly positive for LYVE-1 (Fig. 5F; Supplementary Material, Fig. S8E). These results indicate that *Braf*^{Q241R/+}; *Cre* embryos show defective lymphatic development from the cardinal vein, leading to distention of the JLSs, dilated lymphatic vessels and edema.

Treatment with a MEK inhibitor and/or histone demethylase inhibitors prevents embryonic lethality in *Braf*^{Q241R/+}; *Cre* embryos

MEK inhibitor, PD0325901, treatment is known to rescue the embryonic lethality of Noonan syndrome model mice (24). Pregnant *Braf*^{+/+}; *Cre* mice were treated with various compounds to see whether this would result in recovery from embryonic lethality (Table 2). Male *Braf*^{Q241R} *Neol*^{+/+} mice were crossed with female *Braf*^{+/+}; *Cre* mice, and pregnant mice were intraperitoneally injected with dimethylsulfoxide (vehicle), PD0325901 [0.5 or 1.0 mg of body weight (mg/kg)], MAZ51 (VEGFR3 inhibitor; 1.0, 2.0 or 5.0 mg/kg), sorafenib (BRAF, VEGFR, PDGFR multikinase inhibitor; 5.0 mg/kg), lovastatin (HMG-CoA reductase and farnesyl transferase inhibitor; 5.0 mg/kg) or everolimus (mTOR inhibitor; 0.1 mg/kg), daily from E10.5 to E18.5. PD0325901 treatment (0.5 mg/kg) modestly rescued the embryonic lethality of *Braf*^{Q241R/+}; *Cre* mice (2 of 30). Seven embryos also survived for 3 weeks with